Contributed paper

OPTO-ELECTRONICS REVIEW **10**(3), 217–224 (2002)

Plasmon polaritons in metal nanostructures: the optoelectronic route to nanotechnology

M. SALERNO*[1], J.R. KRENN[1], B. LAMPRECHT[1], G. SCHIDER[1], H. DITLBACHER[1], N. FÉLIDJ[2], A. LEITNER[1], and F.R. AUSSENEGG[1]

[1]Institut for Experimental Physics, Karl-Franzens-University Graz and Erwin Schrödinger Institute for Nanoscale Research, 5 Universitätsplatz Str., A-8010 Graz, Austria
[2]Université Paris 7, Interfaces, Traitements, Organisation et Dynamique des Systémes, 1 rue Guy de La Brosse, UPRES-A 7086, 75005 Paris, France

In the light of recent advances in subwavelength optics, the development of optical nanodevices is nowadays conceivable. Among the best candidates to act as the elementary components of such devices are nanoscale structures of noble metals. These materials are capable to sustain resonant electron oscillations (plasmons). This phenomenon gives rise to a spectrally selective optical response and a local field enhancement which can be used in the context of nano-optics. Furthermore, it allows to transduce the optical signals into electrical ones (and vice versa). Here, we demonstrate an optical nanodevice based on plasmon resonances in gold nanostructures. The adequate metal structures were produced by electron-beam-lithography. The basic operating functions of the device, namely signal processing on the nanoscale and its interfacing on the microscale, were experimentally observed in the optical near-field by photon scanning tunneling microscopy. Furthermore, as a numerical method for validation of the near-field observations the Green's Dyadic Technique is pointed out.

Keywords: surface plasmons, noble metals, nanoparticles, nanowires, photonics, optoelectronics, nanodevices.

1. Introduction

Under proper excitation, noble metal structures can exhibit strong collective oscillations of the conduction electrons, generally termed plasmon resonances [1]. In particular, plasmon modes can be sustained in thin films, called surface plasmons (SPs), and in nanoparticles, called localised SPs or particle plasmons (PPs). While these modes present no fundamental differences with the volume plasmons of basic physics textbooks, the different boundary conditions that apply to the Maxwell equations give rise to a geometrically determined behaviour. This effect is as important as the dependence on the optical constants of the metal structures and their environment [2,3]. SPs and PPs can be conveniently excited in metal structures by an incident light field. In fact, plasmon fields at optical frequencies differ from freely propagating light just because these electromagnetic modes are bound to the interfaces of the metal structures with the surrounding dielectrics, to form a so-called polariton. SPs can propagate along the interface, while PPs correspond to dipolar or multipolar excitations bound to a particle. However, for both modes the field intensity is decaying exponentially on moving away from the interface perpendicular to it, with different decay lengths on the two sides of the interface. From the point of view of optics we speak of near-field (NF) confinement, in contrast to propagating light that extends in the so-called far-field (FF) domain, the border between these two regimes being set by the wavelength of light. Indeed, in conventional FF optics the diffraction threshold of $\sim\lambda/2$ places a fundamental constraint to light field manipulation and transport, as for example the limit on the highest possible resolution of optical microscopy [4]. However, in principle a light NF close to a metal surfaces can still be converted into FF propagating light thanks to frustration of the evanescent light field by approaching an appropriate medium. This is actually the method used in scanning NF microscopy for light detection by an optical fibre tip. Therefore we think that NF localisation of light fields via the plasmon modes bound in the sustaining metal structures can be of great technological relevance for the miniaturisation of optical devices.

In this work we propose to process and transfer a light signal in and along material structures of sub-diffraction limit size, taking advantage of the mediation of plasmons in metal nanostructures. As nanostructures we mean objects with size smaller than the diffraction limit in the visible, i.e., of a typical size around 100 nm. Whereas this is still far from the chemical world of molecules, it can be correctly called nanoscale technology from the point of view of optics. We present optical NF investigations of gold nanostructures (particles and

*e-mail: marco.salerno@kfunigraz.ac.at

wires) excited at their PP and SP resonances, respectively. The displayed measurements have also been compared with numerical calculations. Our goal is to demonstrate that, when noble metals are used as the material, it is possible to realise nano-optical devices with high integration of components below the diffraction limit. This work fits with the current trend of conversion of microelectronics and optoelectronics technology towards systems which are more and more based on just optical principles, finally aiming at the birth of so-called optical computing [5–7]. Mediation of light-matter interaction by plasmon resonances could strongly spur the evolution of a new, integrated technology combining the advantages of both worlds of optics and electronics. The former would be allowed to overcome the current limitations of light processing technology, based on the rules of classical FF optics which restricts miniaturisation of purely optical devices to several hundreds of nanometers. The latter would meet an increase in signal transfer speed and quality compared to microelectronic fabrication principles, as already occurring on a macroscopic scale with dielectric optical fibre wiring.

2. Experimental

For plasmons excited in confined metal structures, both the resonance wavelength and the spatial profile of the local electromagnetic NF enhancement depend on the structure geometry. Therefore a precise tailoring tool is required, enabling control on the individual nanostructure parameters, namely size, shape and orientation. When many nanostructures are present and eventually interacting, control over the relative positions has to be provided as well. Up-to-date, the only fabrication technique that fulfils such requirements is electron-beam-lithography (EBL). We perform EBL on a modified scanning electron microscope (SEM) equipped with additional hardware and software [3]. The process consists of several steps, which are sketched in Fig. 1. As a substrate for our samples glass slides doped with indium-tin-oxide (ITO) are used, to provide the weak electric conductivity needed for EBL operation of the SEM. These substrates are spin-coated with olymethylmethacrylate (PMMA) as a positive electron resist, with a typical thickness of 100 nm. The substrate is then transferred to the SEM, where the sample pattern is imprinted in the resist by means of electron beam exposure. The exposed resist areas are removed by chemical methods, yielding the desired mask, on top of which the metal is thermally evaporated in a high vacuum chamber. Finally, during lift-off the mask is dissolved, removing in turn the evaporated material but in the open areas, where the originally desired metal structure is left. The smallest sample features achievable with this technique are around 30 nm in lateral size, whereas the overall write field size ensuring good pattern uniformity is limited to approximately 200 μm.

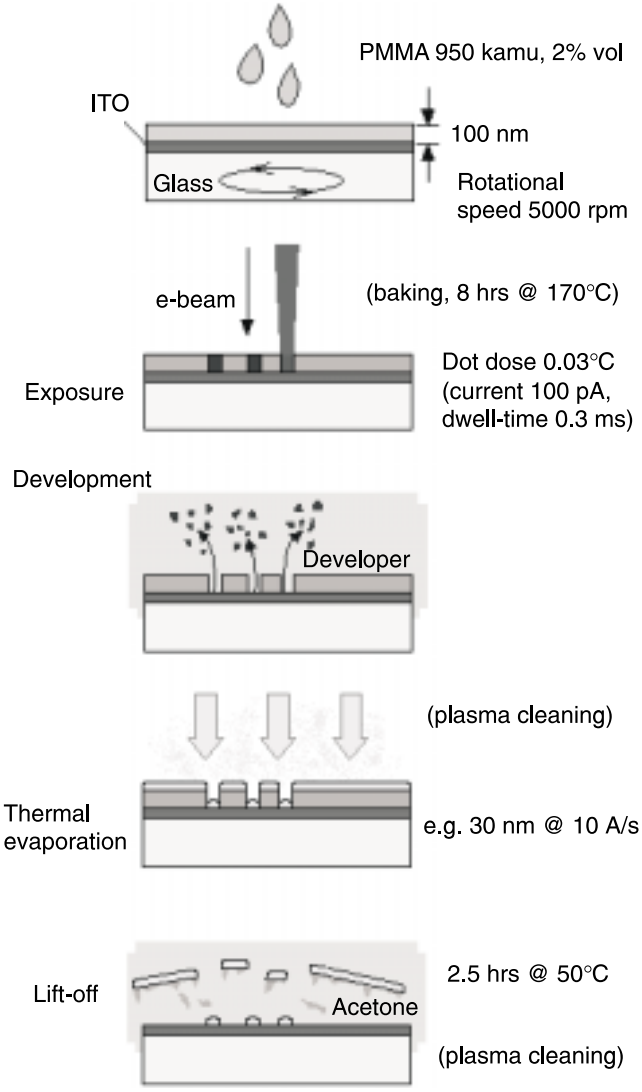

Fig. 1. EBL procedure for fabrication of the patterns of metal nanostructures. For a comprehensive description, see text.

After fabrication the nanostructured metal samples are checked by SEM and atomic force microscopy (AFM) for control of the height of structures. The spectral characteristics are measured by conventional optical extinction spectroscopy. Due to the small overall size of the samples, our spectrometer is coupled to an optical microscope equipped with a low N.A. objective (0.075).

Imaging of the optical NF of the metal nanostructures is performed by a photon scanning tunneling microscope (PSTM) [8], using the scanning and acquisition units of a commercial AFM together with a home-built optical head. The operating principle of PSTM is shortly described with the help of Fig. 2. Total internal reflection (TIR) of a collimated laser beam occurs at the upper surface of the sample glass-ITO substrate, thanks to an optically matched glass prism lying below it, and providing the room for incident and reflected path of the light. In these conditions the sample over the substrate is immersed in an

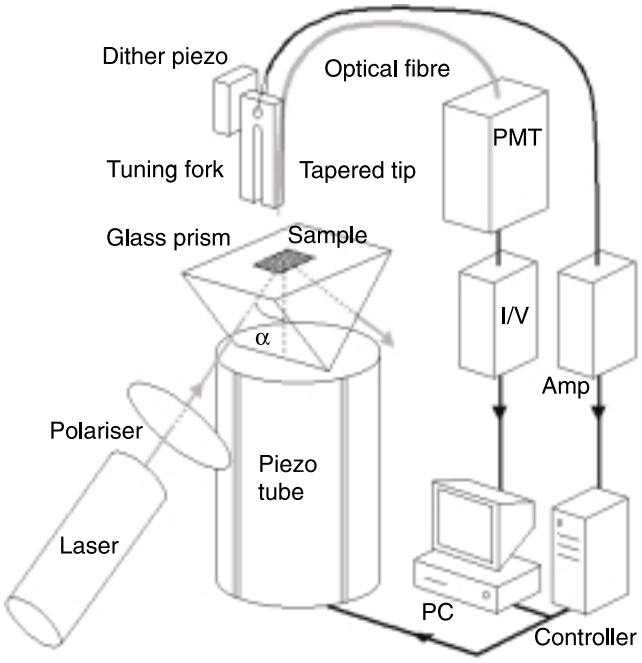

Fig. 2. Sketch of the PSTM setup. α: angle of incidence; PMT: photomultiplier tube; I/V: current to voltage converter; Amp: voltage amplifier.

exponentially decaying evanescent light field which can excite the plasmons in the metal structures while providing a low background illumination. A glass tip is laterally scanned very close to the substrate, frustrating the optical NF of the sample structures. As the object of our investigations are plasmons resonances in metals, different from most scanning NF optical microscope setups a bare (non metallised) optical fibre tip is used, which allows to avoid major perturbations of the imaged fields. This apertureless tip simply works as a scattering centre of the NF of the sample at the tip apex, and part of the scattered light is converted into a propagating light signal which is collected and carried to a FF detector by means of the optical fibre.

The tip is scanned either in constant height or constant distance mode. In the latter case, as the distance dependent signal the amplitude of oscillation of a quartz tuning fork dithered at its resonance is used [9,10]. The optical fibre is glued close to its free end to one arm of the tuning fork. This oscillating system is therefore damped as the tip is approaching the sample, due to shear-force interaction with its surface [11,12].

The tips used in the PSTM measurements were produced by tube etching procedure [13] on single mode optical fibres, using paraffin oil as the overlayer for the aqueous 40% HF etching solution. Hot (~130°C) concentrated (95–97%) H_2SO_4 was used for successive removal of the fibre polymer jacket. A typical taper apex size of approximately 100 nm in diameter is routinely obtained by this method, with a taper cone half angle in the range of 12° to 15°.

3. Theory

The experimental PSTM images of the optical NF of the metal nanostructures were compared with maps of the square modulus of the electric field above the sample calculated by means of the Green's Dyadic Technique (GDT) [14]. This method is based on a discretisation of the modeled objects in the real space. Previous studies have established such GDT maps to be a reliable description of the interaction of light with nanoscale metal structures [15,16].

For the calculations performed in this work, cubic cells with side length of 10 nm were used. The dielectric constant of gold was taken from Ref. 17, while for the substrate an effective dielectric constant of 2.37 was used, accounting for the ITO diffused layer on top of the bare glass substrate plate. The illumination conditions follow from the corresponding experimental parameters.

4. Results and discussion

4.1. Particle plasmons

We begin this section by discussing two examples of metal nanoparticle samples fabricated by EBL. The inset in Fig. 3(a) shows a SEM micrograph of a square grating of oblate (i.e., disk-like) gold nanoparticles, 40 nm in height and 110 nm in diameter. The optical extinction spectrum of this pattern is given by the leftmost curve plotted in the figure, for normal incidence of the exciting light on the substrate plane and linear polarisation along x. The spectrum reveals a PP excitation peak at a 710 nm wavelength. By increasing the particle diameter d in discrete steps up to 180 nm, the resonance wavelength shifts up to 860 nm, as shown by the other reported spectra. The extinction peak height is also increasing, due to the higher overall extinction cross-section of the particles upon particle size increase. In the same way it is possible to tune the resonance of our samples across the whole visible spectral range [2,3].

In Fig. 3(b), on the other hand, particles with elongated cross section parallel to the substrate plane are shown. The dimensions of these prolate (i.e., cigar-like) particles are 120×80×40 nm^3. Such a pattern exhibits dichroic extinction properties, with PP resonance peaks at 770 and 650 nm for polarisation of the exciting light beam along the long (x) and short (y) particle axis, respectively. Additionally, the spectrum acquired for unpolarised exciting light, showing a combination of both polarisations, is plotted in the dashed trace.

Obviously, it is possible to operate on other geometric parameters, as orientation of elongated particles, particle center-to-center distance (i.e., grating constant) in both x and y in-plane directions, or more complex, eventually asymmetric shape of the individual particles, so to tailor the optical response to the desired properties.

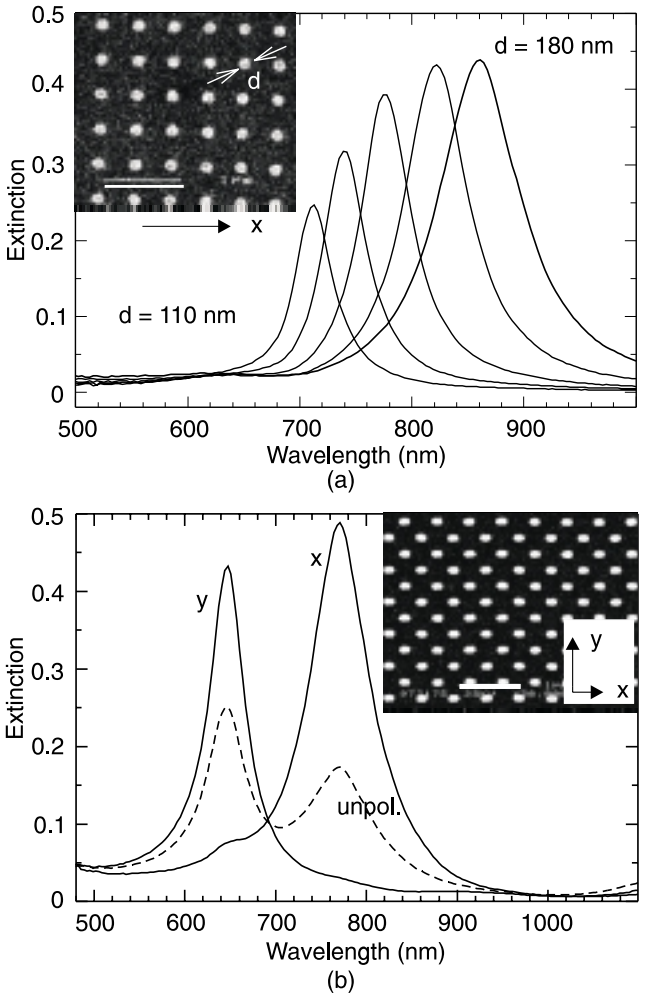

Fig. 3. FF optical properties of typical samples of gold nanoparticles. The plotted curves are extinction spectra, while the insets are SEM micrographs. In (a) the spectra of square gratings of oblate particles are shown. Particle height: 40 nm; particle diameter d increasing from left (d = 110 nm, image in the inset) to right (d = 80 nm). In (b) the case of prolate particles is shown (SEM image bar length 1 μm), exhibiting dichroic behaviour: exciting with light polarized along the long particle axis x yields longer resonance wavelength than using light polarized along the short axis y. (Dashed curve: spectrum for unpolarized light).

The extinction spectra represent the FF optical response of our samples, which tells us about the spectral position of the PP resonance of the individual metal nanostructures. Complementary, as a prerequisite for the study of the NF coupling of closely packed nanostructures, it is necessary to investigate their NF optical response on the sample substrate plane, yielding the field distribution in their close proximity. In Fig. 4, the NF intensity mapped by PSTM is shown for a single gold particle, with a diameter of 100 nm and a height of 40 nm. The particle is resonantly excited with a laser beam of vacuum wavelength $\lambda_0 = \lambda_{PP}$ = 633 nm. In the PSTM, as the exciting light field is provided by TIR, the incident beam is not normal to the sample substrate but inclined at the angle α. In this case $\alpha = 60°$ and the projection of the incident light wavevector on the substrate plane, $k_{||}$, is as shown in Fig. 4(a) (roughly bottom to top in the image). In Fig. 4(a), a diffraction pattern of standing waves is clearly visible, generated from the light incident on the particle and backscatterd from it. Close to the middle of the pattern two higher intensity lobes stand out, characteristic of the incident polarisation state [16,18]. The results of the corresponding GDT calculations are reported in Fig. 4(b), showing a good agreement with the PSTM measurement. The simulation allows to deduce the particle position compared to its NF optical response pattern, represented by a white square. The same information was also obtained from the shear-force topographical map acquired simultaneoulsy with the NF signal when working in constant-distance mode (not shown here). From these images we conclude that the PSTM allows direct mapping of the electric field intensity around the metal nanostructures, as confirmed by theoretical calculations. The same holds also for the case of TE-polarised exciting light, not shown here for the sake of brevity.

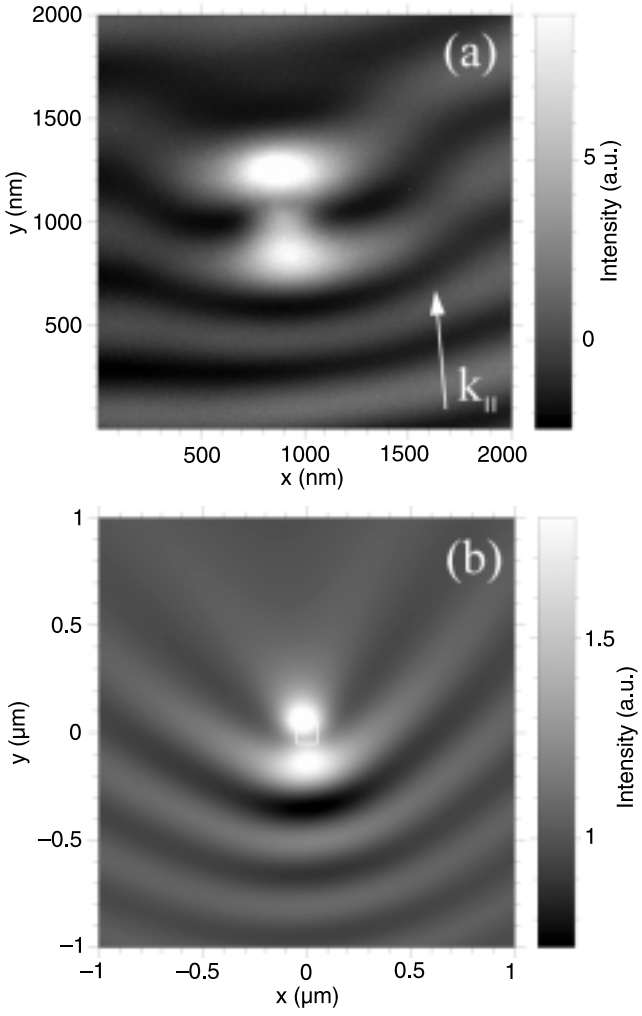

Fig. 4. Optical NF of a PP resonantly excited single gold nanoparticle. Illumination conditions: $\lambda_0 = \lambda_{PP}$ = 633 nm, TM-polarization, $\alpha = 60°$; $k_{||}$ projection of the incident wavevector on the substrate plane. (a) PSTM measurement; (b) GDT simulation.

4.2. Optical nanodevice I: signal processing

As to the technological applications, the PP resonances have already been employed since a long time in optical filters, and their use has also been demonstrated in the field of data storage [19]. Further, recent applications include biomedical analysis [20] and signal enhancement in molecular spectroscopy [21]. Next, we are going to show the feasibility of optical nanodevices based on their properties.

A nanodevice can be defined as a nanoscale size object which possesses two properties: first, the capability of performing operations, e.g., switching on and off elements inside the device; second, the capability of transporting the processed signal, both to connect the device to other similar units close around, and to interface it with the macroscopic world outside. For an optical nanodevice the signal is obviously light, where device operation occurs in the optical NF domain, while connection to the outer world means converting the NF optical signal into propagating light following standard FF rules. An optical nanodevice is therefore equivalent to a nano-optical device, to this extent.

An example of fulfillment of the first task mentioned above is demonstrated in the following experiment. In Figs. 5(a) and 5(b), again the results of PSTM measurement and GDT simulation for a special arrangement of gold nanostructures are shown, respectively. The geometry is as described in Fig. 5(b), where white rectangles represent the position and the approximate shape of the nanostructures. A gold nanoparticle *A* (*x* size 60 nm, *y* size 120 nm, height 40 nm) is directly excited at its PP by the incident light beam (λ_0 = 740 nm, TM-polarisation, α = 60°). Another gold nanostructure, namely a nanorod *B* (*x* size 660 nm, y size 60 nm, height 40 nm) is not excited by the incident light due to its different geometry, but generates just a weak modulation of the surrounding light field background. Obviously the 2-μm distance is such that *B* does not feel the local field enhancement generated from the resonant particle *A*, and can be used as a reference for the behaviour of any similar nanorod when isolated. On the other hand, a nanorod *C* identical to *B* is placed very close to *A*, in its optical NF (around 10 nm distance). In this conditions, on *C* a light field intensity similar in structure to the expected response of *A* (compare with Fig. 4) but extended over the long nanorod length is observed. Clearly the nanorod is also excited, thanks to its proximity with the directly excited *A*. This means that *A* worked as a nanoscopic light source for excitation of *C*, and a signal transmission occurred between the two objects, originated from the PP field of *A* and transferred to *C* by means of optical NF coupling.

In fact, electromagnetic coupling of the dipolar fields of the individual polarised nanostructures can also take place for distances on the order of 1 μm, which is obviously FF in character. As a consequence, in large ensembles of regularly arranged nanostructures a collective behaviour can show up, which strongly modifies the resonance properties of the individual structures in the direction of a red-shift

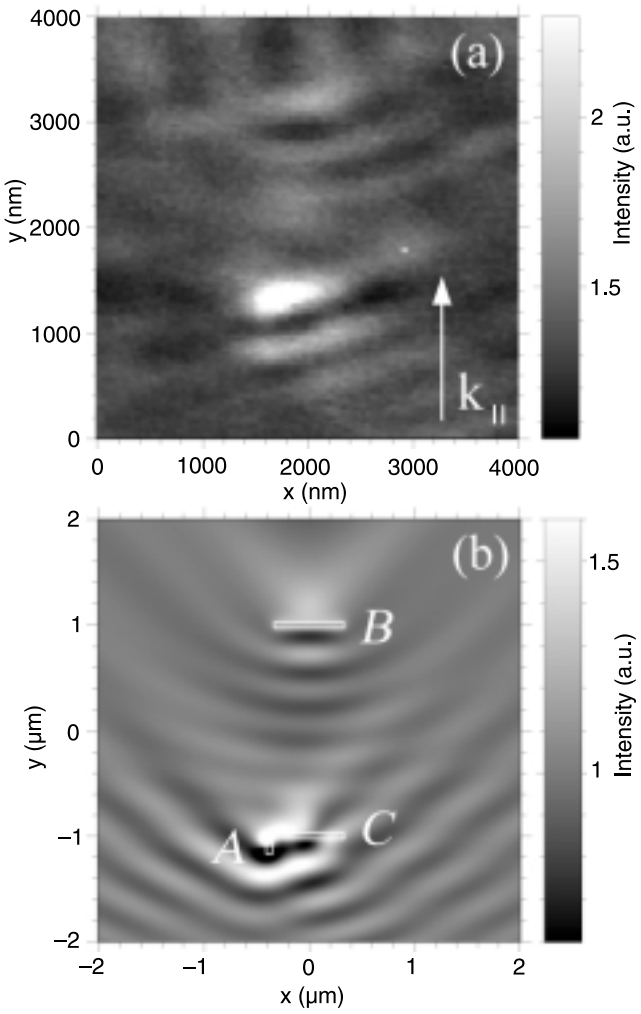

Fig. 5. Optical NF of an arrangement of gold nanostructures, including a PP resonant nanoparticle *A* and two identical nanorods *B* and *C*, far and close to *A*, respectively. Dimensions are 60×120×40 nm^3 for the particle, and 660×60×40 nm^3 for the rods. Illumination conditions: $\lambda_0 = \lambda_{PP}$ = 633 nm, TM-polarization, α = 60°; $k_{||}$ projection of the incident wavevector on the substrate plane. (a) PSTM measurement; (b) GDT simulation.

and a broadening of the PP resonance [22]. This effect has to be kept in mind when designing an optical nanodevice, as it can disturb packing of elements and units inside it.

The described example of light coupling shows that by means of properly arranged metal nanostructures manipulation of light on the nanoscale is possible, such that one could indeed use these structures as the elementary bricks of the optical nanodevice. However, the problem of how to address locally these nanostructures with the light signal, providing the required resolution and in a controlled way, is left. This point is discussed in the next section.

4.3. Optical nanodevice II: signal transport

After (or before) light signal processing inside the optical nanodevice, one needs to interface the device with the exterior user (or driver) to provide an output (or an input, re-

spectively). One possibility to perform this function is by exploiting the capabilities of SPs, in this case. The difference with PPs is that SPs occur in extended metal structures and can propagate along their support relatively far from the excitation region. A propagation length L is defined for SPs, as the in-plane distance at which the SP field intensity, which is exponentially decaying, is reduced to a factor $1/e$ (e is the Neper number). Obviously, for an efficient signal transport a lateral spatial confinement of the SPs into stripes or wires is necessary.

In a former work a FF study of propagation distance of SPs on relatively wide stripes, in the range of some micrometers width (called microstripes), was performed [23]. As expected, for decreasing stripe width w a decreasing propagation length L showed up, leading, e.g., for silver, from >50 to <10 μm L, when decreasing w from 30 to 0.5 μm. While these experiments were based on FF methods, for investigation of further miniaturised SP metal light waveguides a NF optical method was necessary, allowing resolution beyond the diffraction limit. For this reason a PSTM has been used in this work. Our goal was to check the possibility to connect the quasi 0-D elements formed by PP resonant nanoparticles to the SP modes of a 2-D metal film, by means of a 1-D structure which we call a nanowire.

First of all, observation of light transport requires a clear distinction between the excitation region, where the SPs are launched in the metal, and the measurement region. While for wide stripes beam focusing could be used for this task [24], for narrow stripes which give short L a more accurate method had to be developed. We used an integrated thin film system [23], as described in the following. A 3-μm wide gold microstripe acts as the primary medium for SP excitation, by the Kretschmann technique [1] ($\lambda_0 = \lambda_{SP}$ = 800 nm, TM-polarisation, $\alpha = 42.0°$), with the incident wavevector from left to right as indicated by $k_{||}$ in Fig. 6(b). The stripe climbs up a smooth step of a previously deposited layer of an opaque material (50-nm thick aluminum) prepared by shadowed evaporation. This blocks direct light injection in the measurement region which is the area shown in the topographical sample image in Fig. 6(a). Between the aluminum screen and the gold stripe a spacing layer of 50 nm thick SiO_2 is placed, to prevent direct contact.

As we already knew that the SP mode is successfully coupled into the wide microstripe on the left [23], the critical point was to see if the same holds for the much thinner nanowire on the right. In order to address the nanowire with the stripe SP we confined the SP into it progressively, by means of a tapered structure with flat edges [see Fig. 6(a)]. The taper joins the two running plasmon mode regimes, quasi 2-D SP in the microstripe and quasi 1-D SP in the nanowire, working as a "lens".

The corresponding PSTM image is displayed in Fig. 6(b). We observe some light scattering at the edges of the taper, due to SP funneling across it. This is not a problem as far as enough field intensity is still reaching the nanowire, which is clearly the case. A more detailed analysis of the NF distribution of Fig. 6(b) can be done by looking at the longitudinal and transversal profile of the nanowire. The high optical NF resolution allows to detect a spatial modulation of the light intensity, convoluted with the trend of exponential decay. This pattern can only be explained as the interference between forward propagating and backscattered SP waves. Indeed, despite some irregularities probably due to surface defects of the nanowire, a period of 390 nm is measured, which well fits to the $\lambda_{SP}/2$ periodicity of a standing wave pattern. This is a clear demonstration that our metal nanowire is really sustaining a SP mode. Additionally, a large bright spot S is found at the free end of the nanowire, due to SP scattering at the discontinuity.

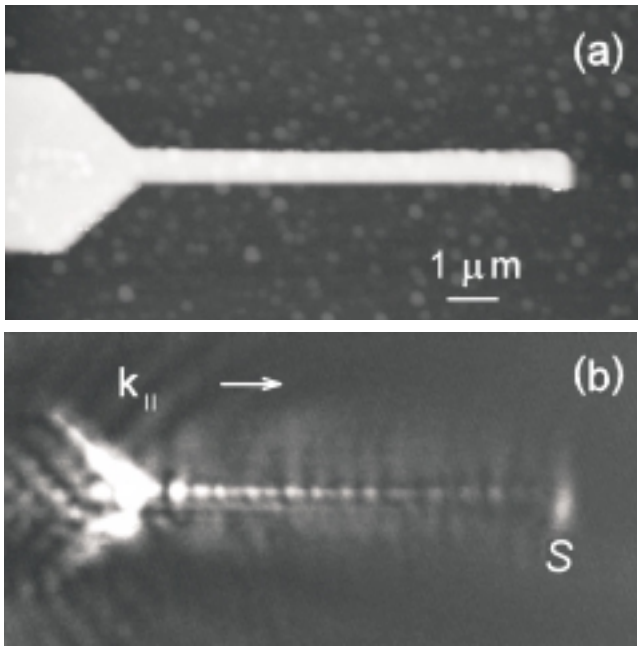

Fig. 6. A gold microstripe tapered down to a nanowire. Gold thickness: 50 nm; stripe width: 3 μm; wire width 200 nm. (a) shear-force topography, acquired simultaneously with (b); (b) PSTM measurement, (illumination conditions: $\lambda_0 = \lambda_{SP}$ = 800 nm, TM-polarization, α = 42°, injected light direction left to right). Image size: 15×7 μm^2. The letter S marks SP scattering at the nanowire termination.

The observed propagation length L of approximately 2.5 μm seems enough for connections inside a nanodevice or between adjacent nanodevices, while for interfacing standard optical microdevices on a larger scale wider stripes can be used, easily providing L values of up to several tens of micrometers [23]. Moreover, for operation of the nanodevice in the telecommunication spectral range (near infrared) even longer L (or alternatively smaller w) can possibly be reached.

What makes this result interesting is above all the lateral confinement at which the SP propagation distance is covered. As designed during EBL and checked from SEM micrographs, the nanowire width is 200 nm. We note that this cross-section looks larger in Fig. 6(a), due to convolution of optical fibre tip and sample profile. This lateral con-

finement is found to be about $\lambda_0/4$, clearly below the diffraction limit $\lambda_0/2$. If the wire thickness of 50 nm is also taken into account, an overall cross section of the wire of $\lambda_0/4 \times \lambda_0/16$ shows up, well below the 2-D diffraction limit $\lambda_0^2/4$. Furthermore, the lateral confinement of the optical signal is even better than that of the physical structure itself, as the transversal profile of the nanowire in Fig. 6(b) shows a FWHM of 120 nm. We note that alternative nanometric metal waveguides can be realised, as in the case of regular arrays of holes drilled in a metal film for light propagation perpendicular through the film [25] or 2-D photonic crystals for light propagation on the pattern plane [26,27]. However, in both cases light guiding requires many elements (in a regular arrangement) which are extending far around the light path, and again this limits the possibility of high integration of nano-optical components.

5. Conclusions

We have shown that EBL is an efficient tool for tailoring nanostructured metal patterns, while PSTM can be successfully used for their characterisation in the optical NF with subwavelength resolution. In particular, the NF of an isolated gold particle with size below the optical diffraction limit was presented. Second, NF electromagnetic coupling between two similar individual objects, a directly excited nanoparticle and a non-excited nanorod, was demonstrated. This is a first example of communication in a possible future microintegrated optical circuit. Finally, transport of the light signal over a micrometer scale distance was shown, through waveguides smaller than the optical diffraction limit.

These results are due to the excitation of plasmon resonances in noble metal nanostructures. It is the transformation of light into and from plasmons that allows one to overcome the fundamental diffraction limit of optics, which is not possible for direct light signals. Therefore, these objects exhibit a great potential for control and manipulation of light on a subwavelength scale, and will be likely used in the development of optical nanodevices with high density of elements.

Furthermore, we showed examples of good agreement between PSTM measurements and electromagnetic NF calculations based on the GDT method. As this technique was previously cross-checked against experiments in a variety of cases, we conclude that it can be used as a reliable method for designing the metal patterned nanodevices, depending on the desired optical response. Hence a complete toolbox is ready for the development of optical nanodevices.

On this track we also tested a multilayer thin film system for local excitation, which could be used in a future optical microchip: in this case no careful alignment of focusing lenses etc. is required, but the light can simply be shone on the whole object, and let it come up (or get out) at the appropriate positions, through windows opened in the aluminum screen.

While allowing miniaturisation of current optical microdevices, metal nanostructure devices could on the other hand be the core of a new optical information technology. This would allow to overcome the speed limits connected to electronic devices [28,29], which have almost reached their ultimate evolution stage such that applied research scientists are looking for engineering alternative solutions. Furthermore, controlled routing of light on a subwavelength scale would allow to address individual molecules, with possible applications in photoactive biosensors, fluorescence, SERS, etc.

Acknowledgements

The authors wish to thank the Austrian Ministry of Technology and the Austrian Science Foundation for financial support. Additional support from the European Union (TMR Project NanoSNOM) is also gratefully acknowledged.

References

1. H. Raether, *Surface Plasmons*, Springer-Verlag, Berlin, 1988.
2. W. Gotschy, K. Vonmetz, A. Leitner, and F.R. Aussenegg, "Optical dichroism of lithographically designed silver nanoparticle films", *Opt. Lett.* **21**, 1099 (1996).
3. W. Gotschy, K. Vonmetz, A. Leitner, and F.R. Aussenegg, "Thin films by regular patterns of metal nanoparticles: tailoring the optical properties by nanodesign", *Appl. Phys.* **B63**, 381 (1996).
4. E. Abbe, "Beiträge zur Theorie des Mikroskops und der mikroskopischen Wahrnehmung", *Archiv. f. Mikroskop. Anat.* **9**, 413 (1873).
5. H. Abdeldayem, D.O. Frazier, M.S. Paley, and W.K. Witherow, "Recent advances in photonic devices for optical computing", *Tech. Rep. NASA* – Marshall Space Flight Center, Huntsville, http://science.nasa.gov/headlines/images/ /nanosecond/thepaper.pdf (2000).
6. Y.S. Park, "Recent advances and future trends in modern electronics", *Int. J. High Speed Electr. and Sys.* **10**, 1 (2000).
7. J. Tominaga, C. Mihalcea, D. Büchel, H. Fukuda, T. Nakano, N. Atoda, H. Fuji, and . Kikikawa, "Local plasmon photonic transistor", *Appl. Phys. Lett.* **78**, 2417 (2001).
8. R.C. Reddick, R.J. Warmack, and T.L. Ferrell, "New form of scanning optical microscopy", *Phys. Rev.* B**39**, 767 (1989).
9. K. Karrai and R.D. Grober, "Piezoelectric tip-sample distance control for near field optical microscopes", *Appl. Phys. Lett.* **66**, 1842 (1995).
10. A.G.T. Ruiter, J.A. Veerman, K.O.V.D. Werf, and N.F. van Hulst, "Tuning fork shear-force feedback", *Appl. Phys. Lett.* **71**, 28 (1997).
11. E. Betzig, P.L. Finn, and J.S. Weiner, "Combined shear force and near-field scanning optical microscopy", *Appl. Phys. Lett.* **60**, 2484 (1992).
12. R. Toledo-Crow, P.C. Yan, Y. Chen, and M. Vaez-Iravani, "Near-field differential scanning optical microscope with atomic force regulation", *Appl. Phys. Lett.* **60**, 2957 (1992).

13. P. Lambelet, A. Sayah, M. Pfeffer, C. Philipona, and F. Marquis-Weible, "Chemically etched fibre tips for near--field optical microscopy: a process for smoother tips", *Appl. Opt.* **37**, 7289 (1998).
14. C. Girard and A. Dereux, "Near-field optics theories", *Rep. Prog. Phys.* **59**, 657 (1996).
15. J.C. Weeber, E. Bourillot, A. Dereux, J.P. Goudonnet, Y. Chen, and C. Girard, "Observation of light confinement effects with a near-field optical microscope", *Phys. Rev. Lett.* **77**, 5332 (1996).
16. J.R. Krenn, A. Dereux, J.C. Weeber, E. Bourillot, Y. Lacroute, J.P. Goudonnet, G. Schider, W. Gotschy, A. Leitner, F.R. Aussenegg, and C. Girard, "Squeezing the optical near-field zone by plasmon coupling of metallic nanoparticles", *Phys. Rev. Lett.* **82**, 2590 (1999).
17. D. Palik, *Handbook of Optical Constants of Solids*, Anal. Chem., 1985.
18. M. Salerno, N. Félidj, J.R. Krenn, A. Leitner, F.R. Aussenegg, and J.C. Weeber, "Near-field optical response of a two-dimensional grating of gold nanoparticles", *Phys. Rev.* **B63**, 16542 (2001).
19. H. Ditlbacher, R. Krenn, B. Lamprecht, A. Leitner, F.R. Aussenegg, and J.C. Weeber, "Spectrally coded optical data storage by metal nanoparticles", *Opt. Lett.* **25**, 563 (2000).
20. T. Schalkahammer, A. Leitner, F.R. Aussenegg, G. Bauer, and F. Pittner, "Optical nanocluster plasmon-sensors as transducers for bioaffinity interactions", *Proc. SPIE* **3253**, 12 (1998).
21. R.M. Stöckle, Y.D. Suh, V. Deckert, and R. Zenobi, "Nanoscale chemical analysis by tip-enhanced Raman spectroscopy", *Chem. Phys. Lett.* **318**, 131 (2000).
22. B. Lamprecht, J.R. Krenn, A. Leitner, and F.R. Aussenegg, "Metal nanoparticle gratings: Influence of dipolar particle interaction on the plasmon resonance", *Phys. Rev. Lett.* **84**, 4721 (2000).
23. B. Lamprecht, J.R. Krenn, G. Schider, H. Ditlbacher, M. Salerno, N. Félidj, A. Leitner, and F.R. Aussenegg, "Surface plasmon propagation in microscale metal stripes", *Appl. Phys. Lett.* **79**, 51 (2001).
24. J.R. Krenn, M. Salerno, N. Félidj, B. Lamprecht, G. Schider, A. Leitner, F.R. Aussenegg, J.C. Weeber, A. Dereux, and J.P. Goudonnet, "Light field propagation by metal micro- and nanostructures", *J. Microscopy* **202**, 122 (2001).
25. H.F. Ghaemi, T. Thio, D.E. Grupp, T.W. Ebbesen, and H.J. Lezec, "Surface plasmons enhance optical transmission through subwavelength holes", *Phys. Rev.* **B58**, 6779 (1998).
26. S.C. Kitson, W.L. Barnes, and J.R. Sambles, "Full photonic band gap for surface modes in the visible", *Phys. Rev. Lett.* **77**, 2670 (1996).
27. M.G. Salt and W.L. Barnes, "Photonic band gaps in guided modes of textured metallic microcavities", *Opt. Comm.* **166**, 151 (1999).
28. B. Lamprecht, A. Leitner, and F.R. Aussenegg, "Femtosecond decay-time measurement of electron-plasma oscillation in nanolithographically designed silver particles", *Appl. Phys. B* **64**, 269 (1997).
29. B. Lamprecht, J.R. Krenn, A. Leitner, and F.R. Aussenegg, "Particle-plasmon decay-time determination by measuring the optical near-field's autocorrelation: influence of inhomogeneous line broadening", *Appl. Phys.* B**69**, 223 (1999).

